Hadronic Interaction Vertices Analysis with the ATLAS Detector

EP-ADP Department

CERN Summer Student Project Report

Submitted by: Natasha Mahmood

Supervisors: Dr. Anthony Morley & Dr. Valentina Cairo

CERN Summer Student Session: June-August 2018

Abstract

The ATLAS detector is able to reconstruct hadronic interaction vertices inside the pixel detector, and with the use of information about the energy deposit of secondary hadrons in subsequent layers of pixel detector (dE/dX), the secondary particle species can be identified (pions can be separated from protons and kaons). The goal of this project is to study the properties of secondary hadrons from interactions of primary particles in specific layers of the pixel detector. In particular, to provide information about the species of the secondary particles that may assist in the tuning of the numerical models used to simulate these interactions.

1. Introduction

The ATLAS Pixel detector is able to provide a measurement of the specific energy loss dE/dx for particles. This report presents a study to identify the secondary hadrons from interaction of the primary particles in specifc layers of the pixel detector. By using the measured energy loss of the secondary particles the number of particles for each species can be extracted. The proton-proton collision data sample used to perform the measurements described in this report was collected in 2015 at a centre-of-mass energy of $\sqrt{s} = 13\ TeV$ by the ATLAS detector [1] at the LHC. During this running period, the LHC was operating in a special configuration with a low instantaneous luminosity. In this report, the EPOS MC Event generator [2] is used to simulate minimum-bias inelastic proton-proton collision.

2. ATLAS Detector

The ATLAS (A Toroidal Large hadron collider ApparatuS) detector is centered on one of the LHC (Large Hadron Collider) collision points. Particles produced in the collisions emerge from the center of the detector in all directions. ATLAS has been designed to record the paths and energies of the particles emerging from the collisions.
ATLAS is composed of a series of concentric sub-systems, each sensitive to different types of particles produced in the collisions. The Inner Detector (ID) [3] is closest to the interaction point and measures the trajectories of charged particles. The ID is composed of the Pixel Detector, the Semiconductor Tracker (SCT), and the Transition Radiation Tracker (TRT). The ID operates in a 2 Tesla magnetic field provided by the solenoid magnet. The entire ATLAS detector and the composition of the ATLAS Inner Detector are shown in Figure 1.

2.1 Inner Detector

The inner detector measures the position of charged particles to high precision as they traverse the detector. The inner detector serve as a spectrometer in which the curved trajectories of charged particles can be reconstructed.
The Pixel detector is the closest sub-detector to the interaction point and comprises four barrel layers and two end-caps with three disks each. The ATLAS inner detector is able to provide a measurement of the momentum and specific energy loss dE/dx for particles from proton-proton collision. The momentum and energy loss measurements together can be used to distinguish between different types of the charged particles.

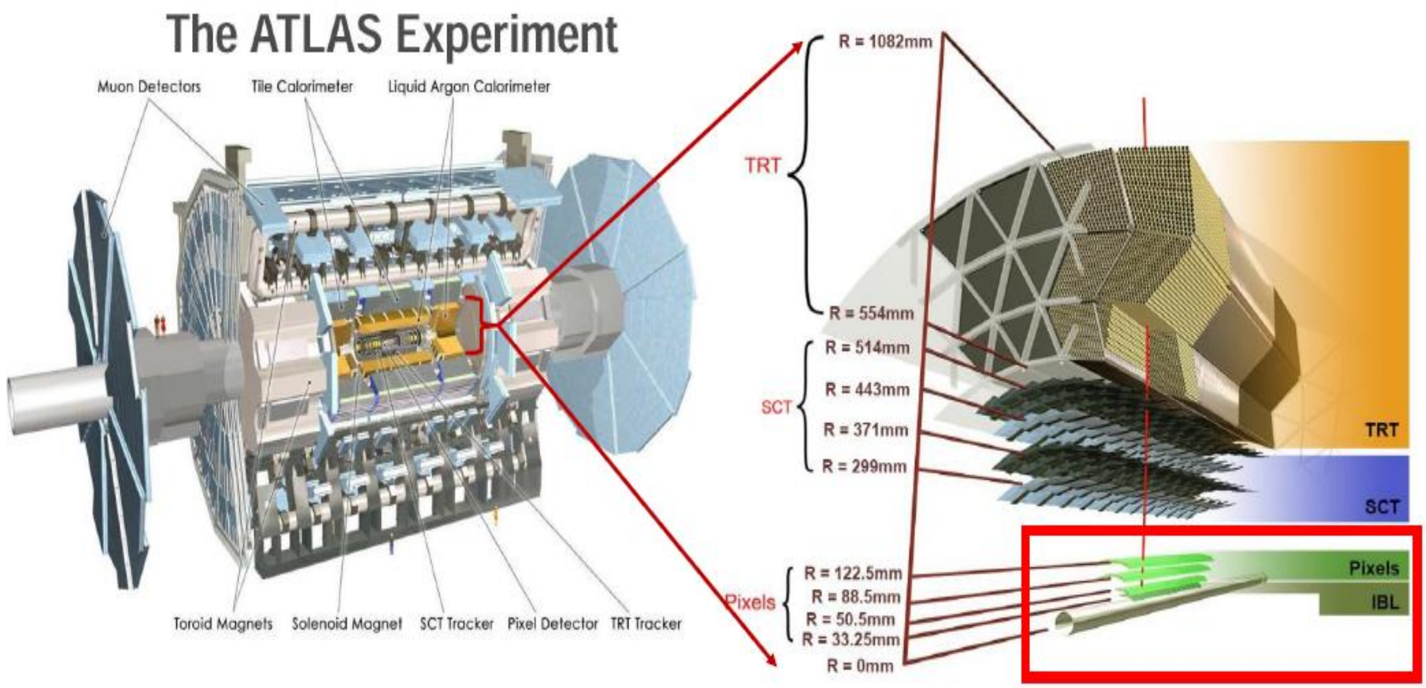

Figure 1: View of ATLAS detector and composition of ATLAS Inner detector

3. Identification of Particles

The various elementary particles give different characteristic signature in the separate detectors that make up the experiment. In particular, we can use information of energy loss in the pixel detector to help distinguish between different charged particles.

The Bethe-Bloch formula provides the momentum dependence of the energy loss of different particles with given mass.

$$< -\frac{dE}{dx} > \; = Kz^2 \frac{Z}{A}\frac{1}{\beta^2} \; [\frac{1}{2} ln \frac{2m_e c^2 \beta^2 \gamma^2 W_{max}}{I^2} \; - \; \beta^2 \; - \; \frac{\delta(\beta\gamma)}{2}]$$

Where, $K = 4\pi N_A r_e^2 m_e c^2$, z = charge number of incident particle, Z = atomic number of absorber, A = atomic mass of absorber, W_{max} = energy transfer to an electron in a single collision, I = mean excitation energy, δ = density effect correction to ionization energy loss

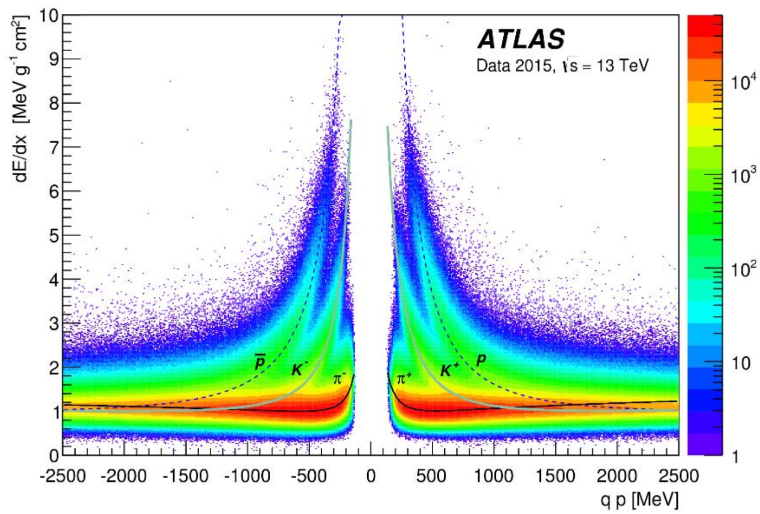

Figure 2: Energy loss distribution as a function of charge and momentum. [4]

We can identify different type of charged particles more precisely at low momentum (~ 200 MeV) but it becomes difficult to identify particles at higher momentum (above ~1500 MeV) as shown in figure 2.

4. Hadronic Interaction

Hadronic interactions are inelastic scattering between hadrons and detector material. When multiple child particles of a hadronic interaction are reconstructed as tracks, it is possible to reconstruct the position of the interaction as the vertex. The radial position resolution of the vertex reconstruction is O(100μm). This enables a precise radiography of the material and the location to be determined of sub-millimeter size detector components. The hadronic interaction analysis aims to identify and reconstruct the vertices of hadronic interactions.

4.1 Events selection

Events are required to have exactly one primary vertex which has at least two tracks with $p_T > 200\,MeV$. Secondary vertices are required to satisfy $|\eta| < 2.5$ where the pseudorapidity is measured with respect to the primary vertex, $|z| < 300\,mm$ and $r > 20\,mm$.
To reject K_S^0, Λ and $\overline{\Lambda}$ decays, originating from in-flight decay vertices, the following requirements are applied for vertices whose associated tracks have oppositely signed charges:

- $K_S^0 \to \pi^+\pi^-$: It is required that $\left|m_{SV}(\pi\pi) - m_{K_S^0}\right| < 0.02\,GeV$, where $m_{SV}(\pi\pi)$ is the so-called secondary-vertex invariant mass, calculated using the track parameters at the vertex. The $m_{SV}(\pi\pi)$ value is calculated assuming pion masses for both tracks, and $m_{K_S^0}$ is the mass of K_S^0 (0.49765 GeV) [5], as shown in figure 3.

- $\Lambda \to p\pi^-/\overline{\Lambda} \to \bar{p}\pi$: It is required that $|m_{SV}(p\pi) - m_\Lambda| < 0.05\, GeV$ where $m_{SV}(p\pi)$ is calculated assuming that the particle with larger p_T is a proton or antiproton, and the other particle is assumed to be a pion, and m_Λ and $m_{\overline{\Lambda}}$ is the mass of Λ and $\overline{\Lambda}$ (1.1156 GeV) [5], as shown in figure 4 and 5, respectively.

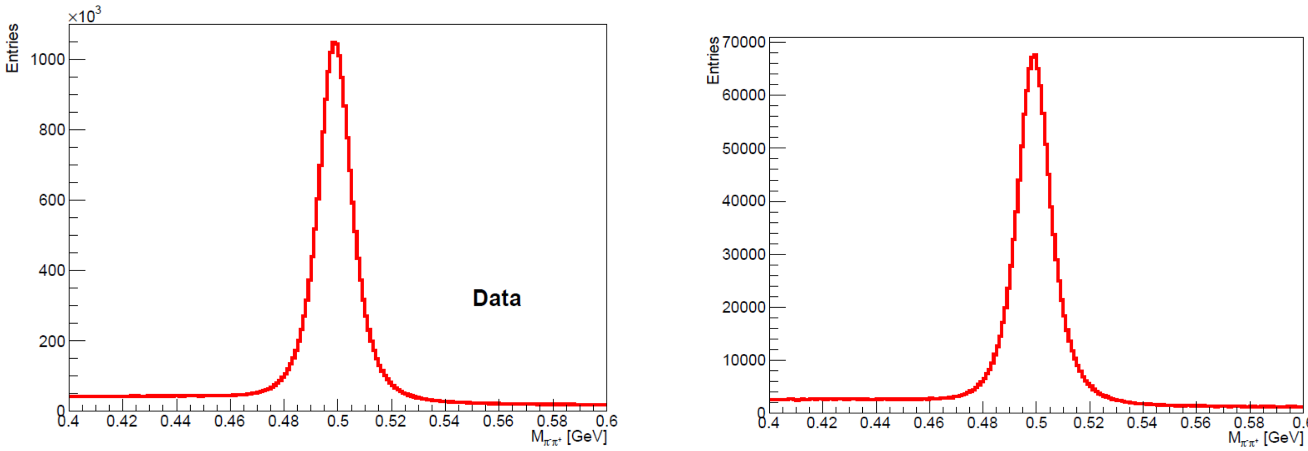

Figure 3: The invariant mass of the K_s^0 decay production in data (left) and simulation (right)

The figure 3 shows the invariant mass of K_s^0 candidates, i.e. pion and anti-pion, in data (left) and MC simulation (right).

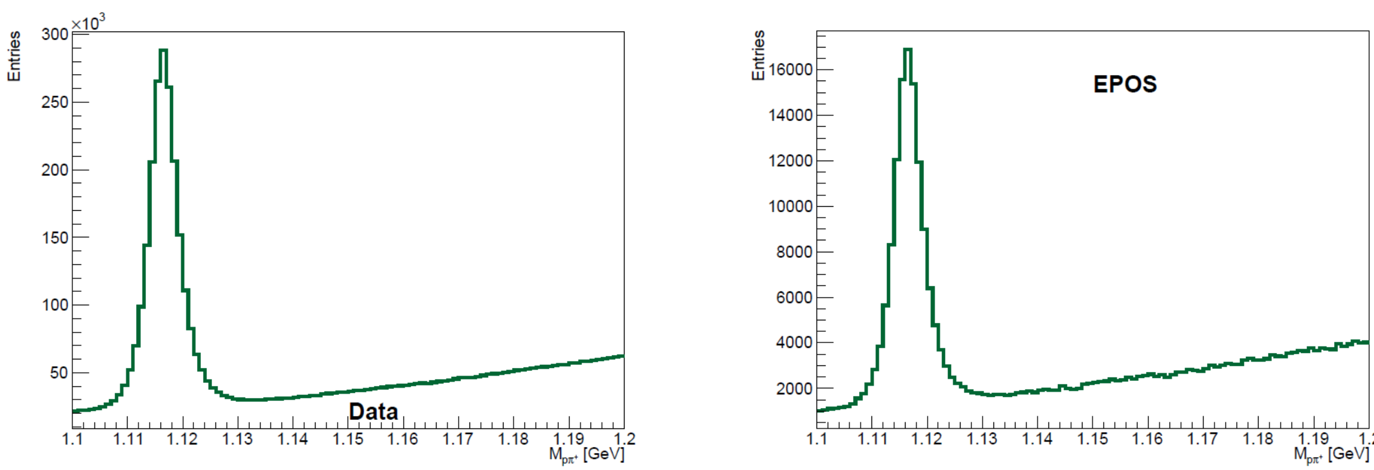

Figure 4: The invariant mass of the Λ decay production in data (left) and simulation (right)

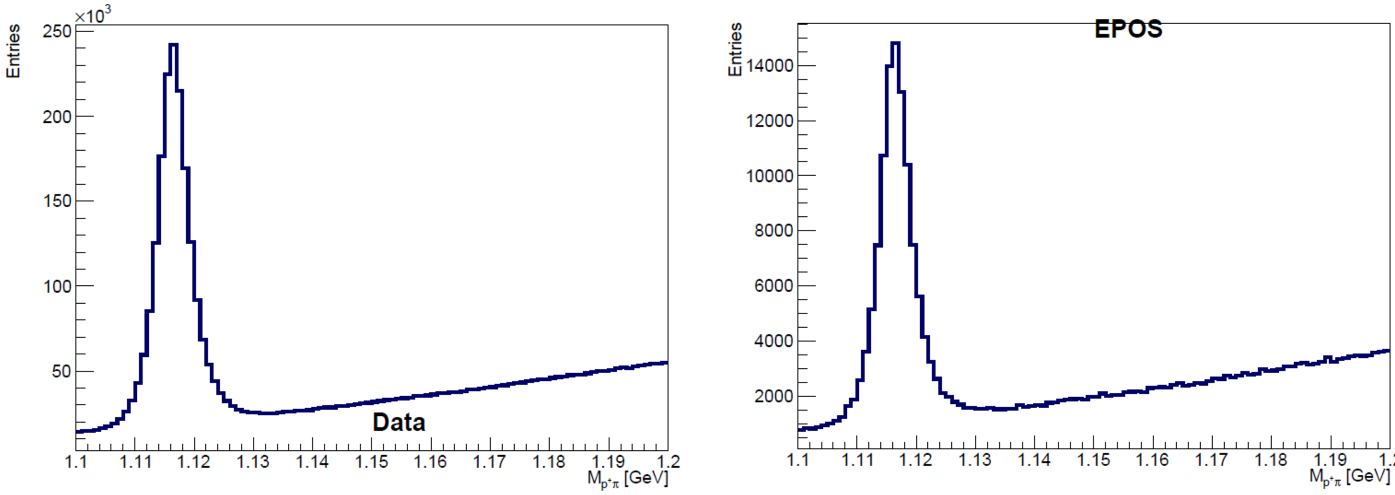

Figure 5: The invariant mass of the $\bar{\Lambda}$ decay production in data (left) and simulation (right)

The invariant mass of Λ and $\bar{\Lambda}$ is same as shown in figure 4 and 5 respectively but the charge is different so are the decay products.

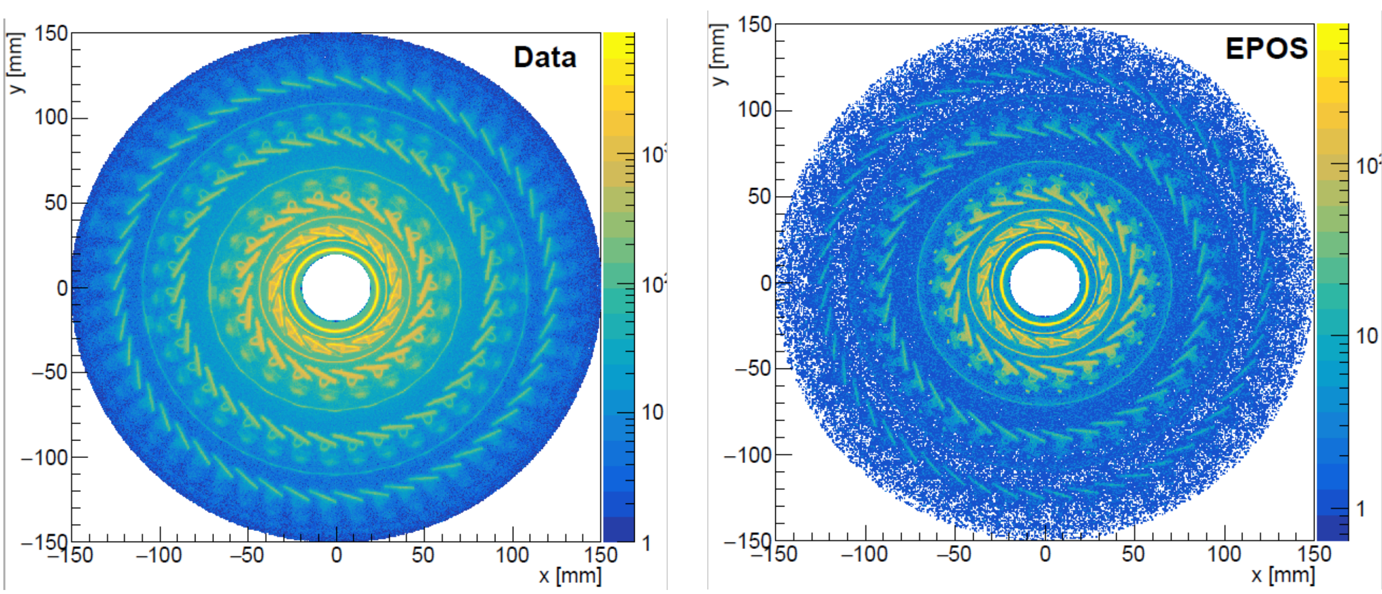

Figure 6: Distribution of hadronic interaction vertex candidates within $|\eta| < 2.5$ and $|z| < 300\ mm$ in x-y view for data (left) and the EPOS MC simulation (right).

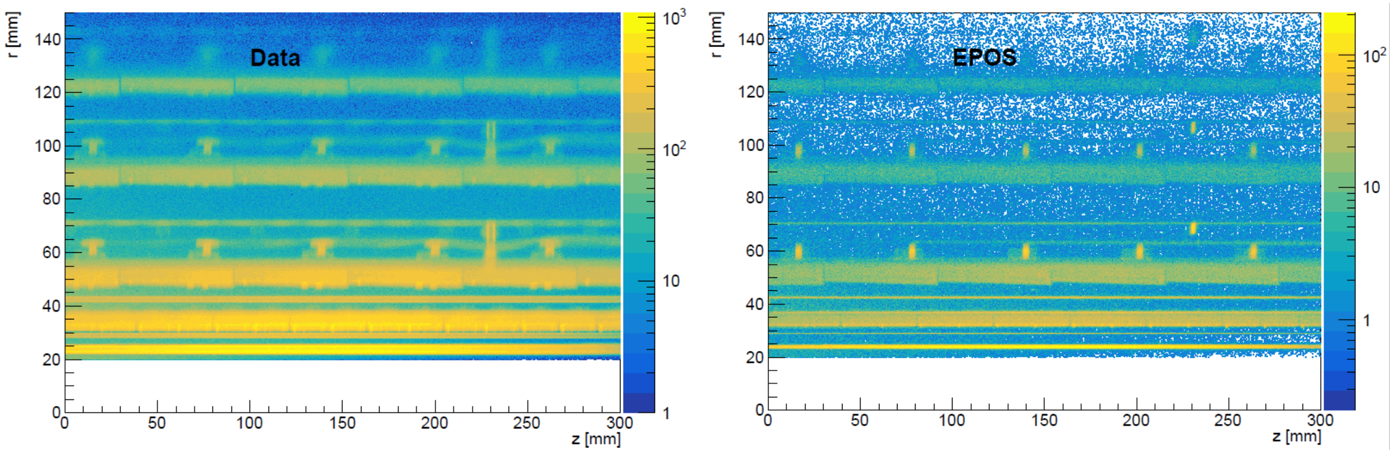

Figure 7: Distribution of hadronic interaction vertex candidates within $|\eta| < 2.5$ and $|z| < 300\ mm$ in r-z view for data (left) and the EPOS MC simulation (right).

By reconstructing the x-y (figure 6) and r-z (figure 7) position of hadronic interaction vertices, we can basically produce radiographies of the ATLAS pixel detector. The excellent radial resolution allows us to see very fine details of the detector e.g. inner barrel layer IBL, supporting tubes, beam pipe etc. Given the excellent radial resolution one can compare data and MC simulation already by looking at the radiographies. The qualitative features of the distributions indicate that the geometry model description is generally accurate.

5. Energy Loss Fit

For a sufficiently large sample of reconstructed tracks from secondary interactions, which have had their dE/dx measured in the pixel detector and momentum, we can plot the correlation of the two quanties as shown in figure 8 (left).

If we divide the sample into momentum slices, a fit to the dE/dx distribution can be performed to extract the number of particles for each species as shown in figure 8 (right).

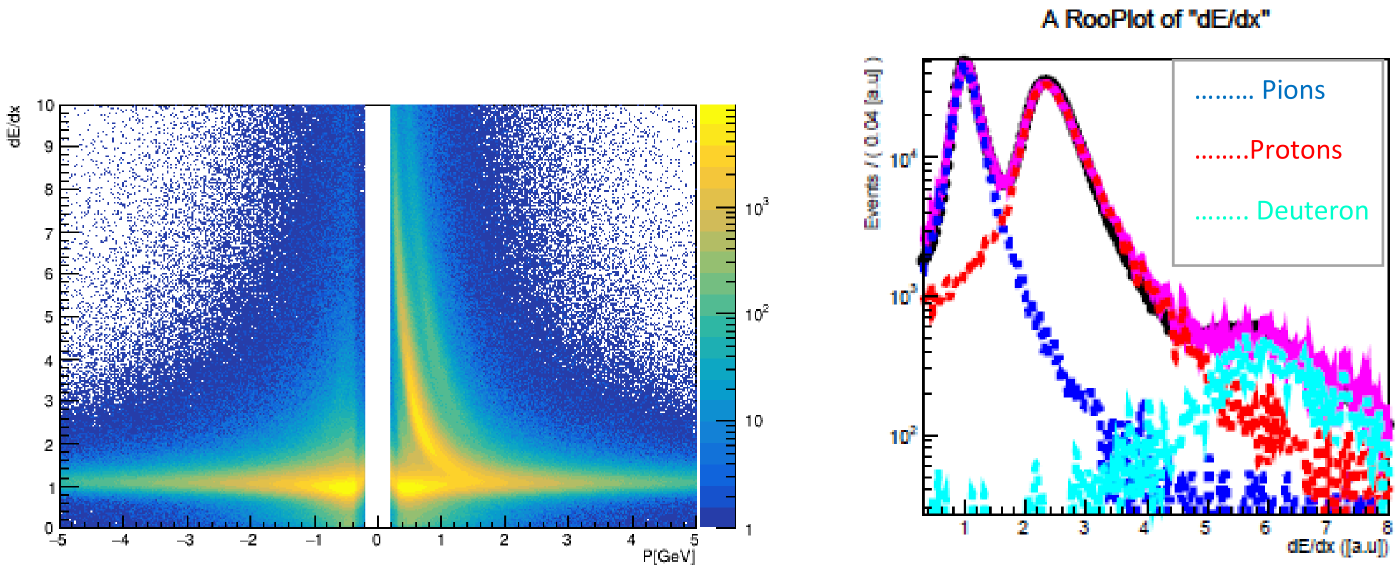

Figure 8: Energy Loss dE/dx distribution as a function of the momentum (left) and an example of the fits of the dE/dx per slice of momentum at 0.70 GeV (right)

To perform the fit to dE/dx distribution the probability distribution function pdf for dE/dx for each particles species is required.
Initially a Crystal Ball function was used to describe this but it was found that the shape was unable to accurately model the data/simulation shapes. (see Appendix A).
The probability distribution function that used to produce the final results was based on the dE/dx shape in simulation which was convolved with a Gaussian. The Gaussian was used to try and account for the small shape difference seen between data and simulation.

6. Results and Discussion

Results of the fitted and truth fraction of particles in simulation are presented in figure 9 and the comparison between fitted fraction of particles in data and simulation is shown in figure 10.

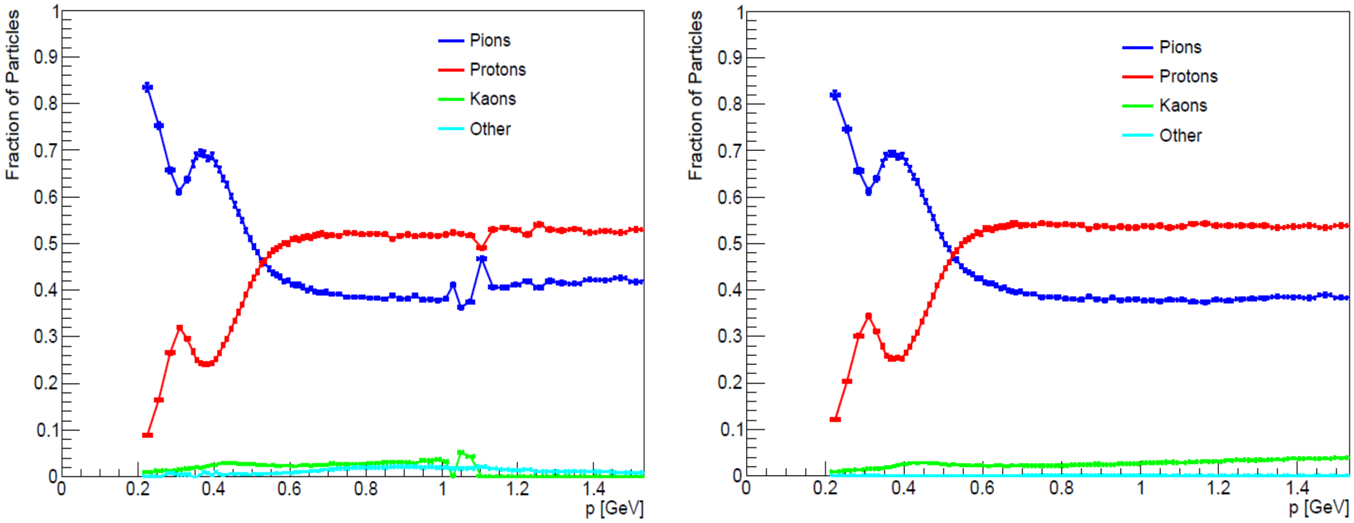

Figure 9: Comparison between fitted fractions of particles from dE/dx (left) and truth fraction of particles (right) in MC simulation.

In figure 9, the truth fraction of particles are compared with the fitted fraction of particles extracted from the energy loss fit to ensure that the fit is reliable.
The fraction of pions dominates the low momentum regime by reaching up ~80% of the total particles and it decreases down until reaching a plateau of ~40% for momenta higher than 0.6 GeV. The fraction of protons has a complementary behavior: it is roughly 10% at low momentum and reaches a plateau value of 50% at higher momenta.

In simulation, the shape of the fraction of particles resulting from the fits are reasonably compatible with those of the truth fraction of particles but some discrepancies are visible. For instance, the plateau value is higher (~3%) in the fitted distributions with respect to the truth ones.

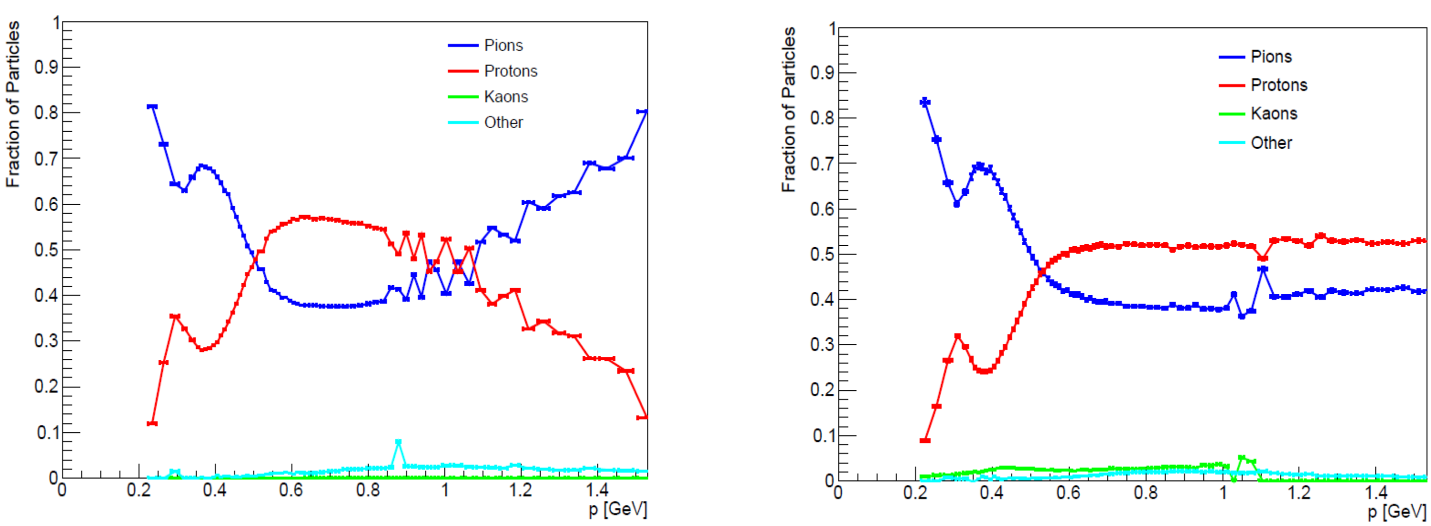

Figure 10: Comparison between fitted fractions of particles in data (left) and MC simulation (right)

In Figure 10, the fit results are compared between data and simulation. At large momentum values the fraction of pions (protons) in data increases (decreases) dramatically rather than reaching a plateau as in simulation. At low momentum values, where it is easier to discriminate between different particles, the shape of the distributions is compatible between data and simulation, but in data the fraction of pions (protons) is ~5% smaller (larger). Further checks will allow to understand if this is an artifact of the fitting procedure, which can be improved, or if there is an actual mismodelling in simulation.

7. Conclusion

Hadronic interaction vertices analysis is used to study the properties of secondary hadrons from interactions in specific layer of the pixel detector. With this work we have demonstrated that it is possible to extract the particles composition in data by fitting the distribution of the energy loss in the pixel detector as a function of the momentum. In the future, the precise measurement of the fraction of particles will allow us to compare data and MC simulation and eventually improve the simulation of particle interactions with matter.

Acknowledgements

I thank **CERN** for arranging Summer Students programme every year and providing a great opportunity for students to work under leading experts in a unique environment. I would like to offer my heartiest gratitude to **Summer Student team** for their guidance.

I express my deep gratitude and respect to my project supervisors **Dr. Anthony Morley** and **Valentina Cairo** from EP-ADP Department for their keen interest, guidance, support, and encouragement during my project.

I am truly grateful to my mentors **Dr. Bilal Masud** director of CHEP institute at University of the Punjab and **Dr. Ashfaq Ahmad** director of EHEP department at National Centre for Physics, Pakistan for referring me and allowing me to avail this opportunity.

8. References

[1] ATLAS Collaboration, The ATLAS Experiment at the CERN Large Hadron Collider, JINST 3 (2008) S08003.

[2] S. Porteboeuf, T. Pierog and K. Werner,
Producing Hard Processes Regarding the Complete Event: The EPOS Event Generator,
arXiv: 1006.2967 [hep-ph].

[3] ATLAS Collaboration, ATLAS inner detector: Technical Design Report, 2.
Technical Design Report ATLAS. CERN, Geneva, 1997.

[4] ATLAS Collaboration (Aaboud, Morad *et al.*) Phys.Rev. D93 (2016) no.11, 112015 arXiv:1604.04520 [hep-ex] CERN-EP-2016-063

[5] The Review of Particle Physics (2018), M. Tanabashi et al. (Particle Data Group), Phys.Rev D98, 030001 (2018).

9. Appendix A

In this appendix, the results of the fits obtained by using a Crystal Ball function are represented. An example is show in figure 11.

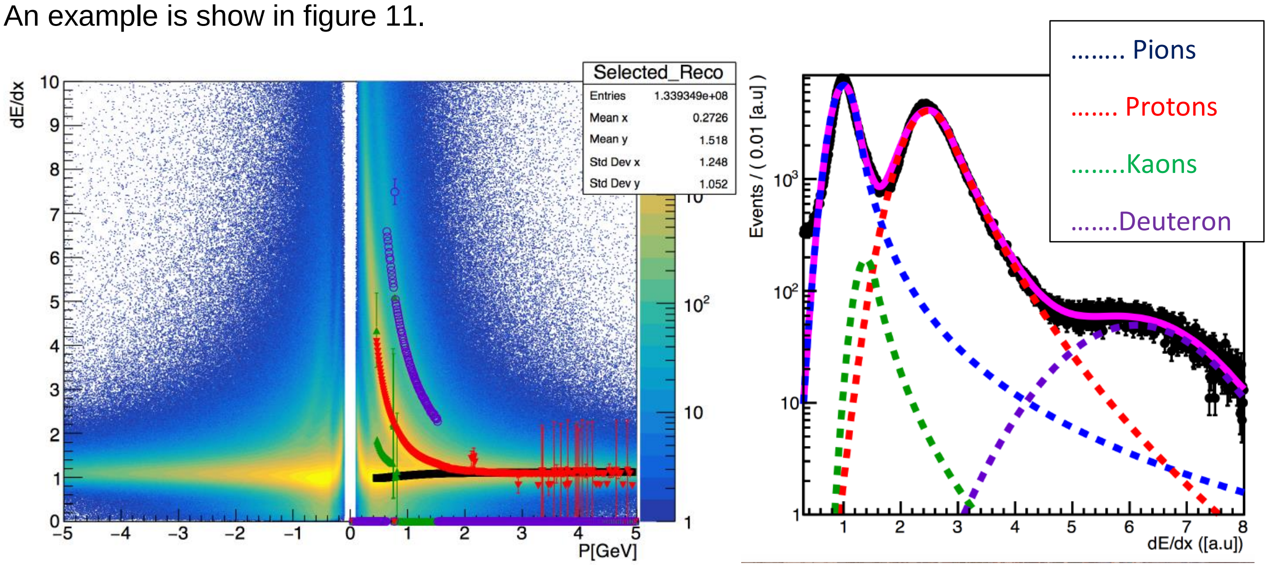

Figure 11: Fit the number of pions, protons, kaons and other particles which are present in sample using Crystal ball function.

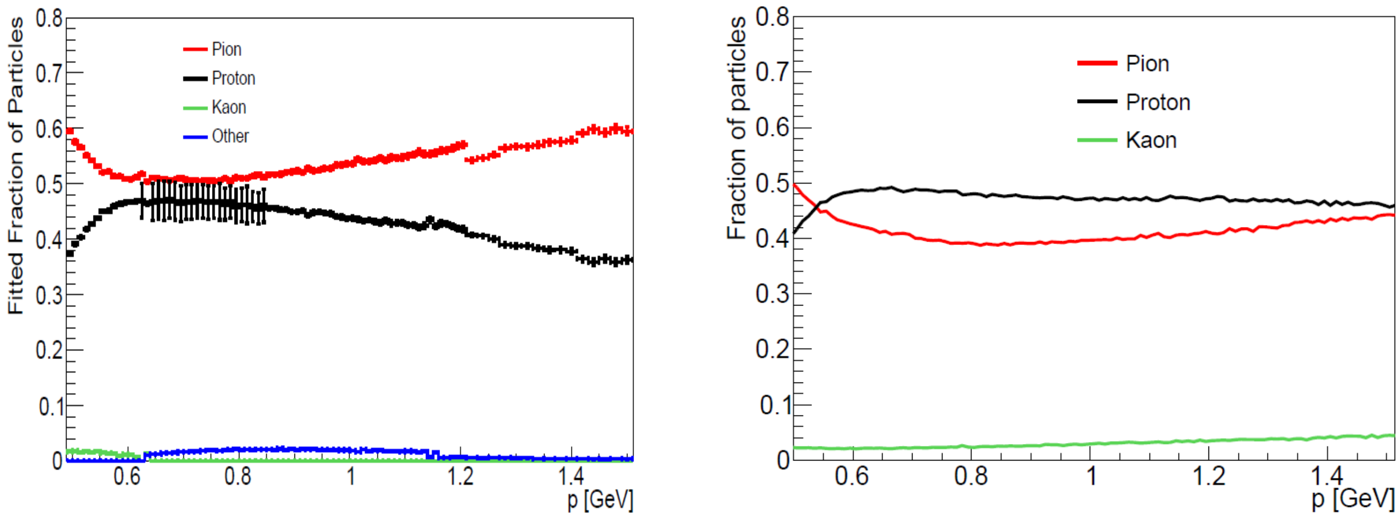

Figure 12: Comparison between fitted fraction of particles from dE/dx (left) and truth fraction of particles (right) in MC simulation

The shapes of the distributions of the particles' fractions obtained from the fits looked consistent with the shapes of the "true" distributions, but a large normalization difference was visible (~10%). The fits overestimated (underestimated) the fraction of pions (protons).

Changing the fit function as represented in main body, allowed to obtained a suitable improvement in the reliably of the fitting procedure.

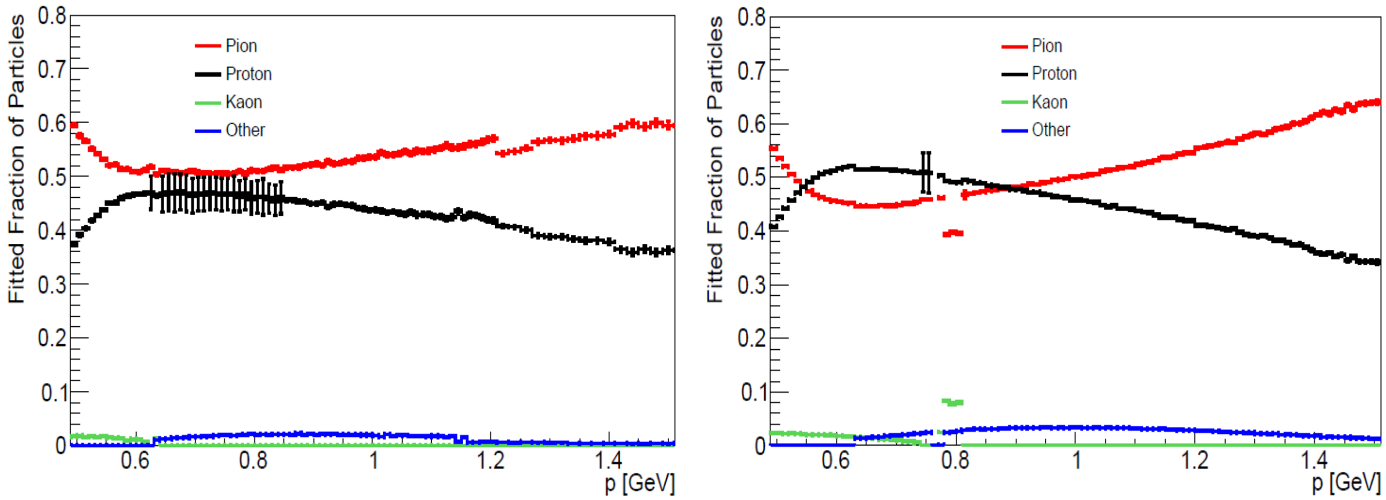

Figure 13: Comparison between fitted fraction of particles from dE/dx in MC simulation (left) and Data (right)

The shapes of the distributions of the fitted fraction of particles obtained from MC looked consistent with the shapes in data, but an overall normalization difference was visible (~10%). The fits overestimated (underestimated) the fraction of pions (protons) in data with respect to simulation.